Comparative Evaluation of a Commercially Available 1.2 kV SiC MOSFET Module and a 1.2 kV Si IGBT Module

S. Tiwari, O.-M. Midtgård and T. M. Undeland
Norwegian University of Science and Technology
7491 Trondheim, Norway
Email: subhadra.tiwari@ntnu.no

***Abstract*—In this paper, a comparative performance evaluation of a 1.2 kV SiC MOSFET module and a 1.2 kV Si IGBT module is carried out under a series of different conditions such as similar dv/dt, di/dt, voltage overshoot, current overshoot, and ringings. Both the modules are commercially available in a standard plastic package and have the same stray inductances. Various parameters such as switching speed, energy loss, and overshoots are experimentally measured in order to address the comparative advantages and disadvantages of the selected modules. This paper demonstrates that SiC MOSFET can replace Si IGBT of similar voltage class or even higher voltage class, both in slow and fast switching applications.**

I. Introduction

The commercially available SiC MOSFETs in a voltage class of 1.2 kV and 1.7 kV can replace Si IGBTs in the same voltage or even higher voltage areas [1], [2], [3], [4]. This is because of the higher breakdown electric field in SiC which allows the use of thinner and shorter drift layer, reducing the capacitances and on-resistances and making the SiC devices suitable for faster switching and higher voltage applications.

There are several publications comparing the switching performances of SiC devices and Si counterparts. For example, a six-pack SiC MOSFET module is compared with a six-pack Si IGBT module keeping similar gate resistance in [5] and under similar dv/dt conditions in [6]. Similarly, a half-bridge SiC MOSFET module is compared with a SiC IGBT module under same dv/dt conditions in [7].

However, few publications have compared the half-bridge SiC MOSFET module against the Si IGBT module under a series of different conditions such as similar di/dt, voltage and current overshoots and ringings, as carried out in this paper. It is important to quantify the switching speed limits of the fast switching SiC MOSFET modules compared to today's fast switching Si IGBT modules. Therefore, in this paper, a commercially available SiC MOSFET module and a Si IGBT module are evaluated by observing their switching performances in all the aforementioned conditions, including also similar dv/dt conditions as in other publications. The selected SiC MOSFET module is CAS300M12BM2 from Cree and the Si IGBT module is SKM400GB125D from Semikron. Each of them have a voltage rating of 1.2 kV, a current rating of 300 A and also similar stray inductances inside the module (L_{module}).

II. Methodology and Laboratory Setup

A standard double pulse test methodology is used for evaluating the stresses, for instance, current and voltage overshoots, ringing, dv/dt, di/dt, and switching energy losses in the device under test (DUT), as described in [8], [9]. An equivalent circuit with a hard switched arrangement is shown in Fig. 1. The total stray inductance in a switching loop (L_{stray}) is the sum of L_{dcbus}, L_{byp}, and L_{module} which are depicted in Fig. 1. L_{module} is the effective stray inductance which is distributed inside the module, represented by red coils.

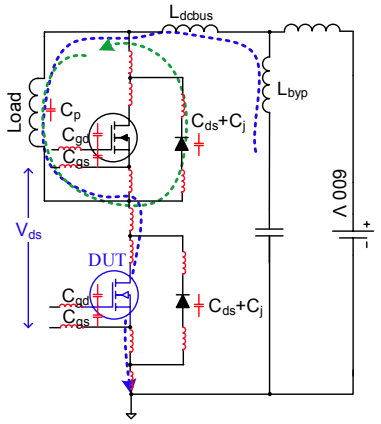

Fig. 1. Current paths show turn-on and turn-off processes in a buck converter during the double pulse test of lower MOSFET. V_{gs} of -5 V is applied in the upper side MOSFET to ensure that it is turned off all the time.

The dc-link is realized with a planar busbar except the termination parts (needed to facilitate the module connection) so that the stray inductance in the switching loop can be kept as low as possible. A current viewing resistor (CVR) SSDN-414-01 (400 MHz, 10 $m\Omega$) from T&M research is used for measuring the drain current. The CVR replaces one of the screws in the SiC module as it is mounted directly on the screw terminal. This arrangement decreases the L_{stray} even further as one screw hole is eliminated in the busbar. L_{byp} and L_{dcbus} are calculated using Ansys Q3D extractor, and is 14 nH in total [10]. The picture illustrating the placement of the CVR in the laboratory setup is shown in Fig. 2.

An inductive load with a single layer winding is used in order to ensure minimum stray capacitance [11]. An isolated

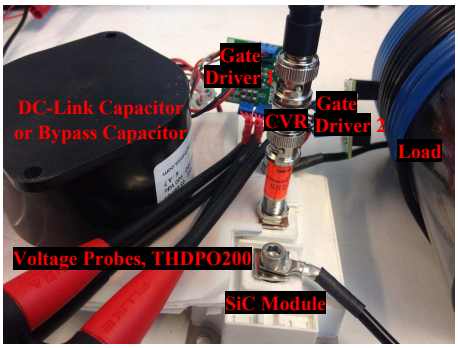

Fig. 2. Hardware setup showing a planar busbar, placement of CVR instead of a screw, several parallel capacitors in the dc-link to reduce L_{byp}, and to realize an overall low L_{stray} in the switching loop. V_{ds} of the lower side MOSFET in the half-bridge is measured across the sources of the upper and the lower MOSFETs.

gate driver with an adjustable output voltage [12] is used for driving the SiC MOSFETs where the gate voltage (V_{gs}) is set to 20 V for turn-on and -5 V for turn-off. The same gate driver is used for driving the Si IGBT with a small modification to achieve the required gate voltage of $\pm$15 V. High voltage differential probes (THDPO200, 200 MHz) are used for drain voltage (V_{ds}) and gate voltage measurements.

Both the modules have been opened to see the internal layout and the distribution of the chips. The Cree module has 6 co-pack MOSFETs in each of the upper and the lower sides in the half-bridge configuration. In the Semikron module, there are 4 co-pack IGBTs in each of the upper and the lower side switches. SiC MOSFET has SiC Schottky barrier diode (SBD), while Si IGBT has Si pn diode as an anti-parallel diode. The opened modules are displayed in Fig. 3.

The typical characterizing parameters such as die size, input capacitances (C_{iss}), output capacitances (C_{oss}), and reverse transfer capacitances (C_{rss}) (sometimes called Miller capacitances) of the modules are listed in Table I [13], [14]. The gate charge (Q_g) is 1025 nC in the MOSFET and 2650 nC in the IGBT. The higher Q_g increases the cost of the gate driver circuit.

Each die in the Cree module has thickness of 200 μm, and area of 26 mm^2, while the thickness is 180 μm and area is 122 mm^2 in the IGBT module [15], [16]. The total die size in Si IGBT is larger by a factor of 3 compared to SiC MOSFET. In addition, Si has higher dielectric constant than SiC. Both of these factors lead to a larger capacitances in the Si IGBT compared to the SiC MOSFET module. (A dielectric constant in Si is 11.9, while it is 10 in 4H-SiC.) An electrical breakdown field of 10 times higher in SiC compared to Si allows thinner and shorter drift layer. However, the thickness of chip and area is a trade-off between on-state resistance (R_{dson}) and capacitances of the power MOSFET structure.

R_{dson} in the MOSFET is 5 mΩ at 25 °C and 7.8 mΩ at 125 °C. In the Si IGBT, R_{ceon} is 6.3 mΩ at 25 °C and 7.6 mΩ at 125 °C. In addition, the Si IGBT has an on-state zero-current collector-emitter voltage (V_{CEO}) of 1.4 V at 25 °C and 1.7 V at 125 °C. Using these parameters, the on-state power losses

(a) Internal layout of CAS300M12BM2 (Cree).

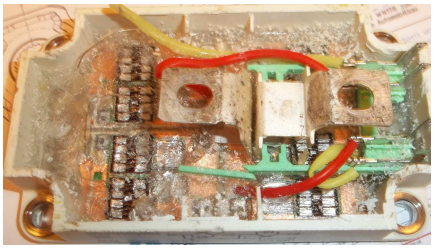

(b) Internal layout of SKM400GB125D (Semikron).

Fig. 3. Picture showing the number of chips and internal layout of modules.

TABLE I
DIE SIZE AND CAPACITANCES OF HALF-BRIDGE MODULES USED IN THE MEASUREMENT

Parts Half-bridge	Die size (mm x mm)	C_{iss} (nF)	C_{oss} (nF)	C_{rss} (nF)
CAS300M12BM2 (Cree)	4.04x6.44	11.7	2.55	0.07
SKM400GB125D (Semikron)	11.08x11.08	22	3.3	1.2

TABLE II
NUMBER OF CHIPS, FORWARD VOLTAGE DROP AND THE RECOVERY OR CAPACITIVE CHARGE OF ANTI-PARALLEL DIODES IN THE MODULES

Parts Half-bridge	Chips (N x)	V_{FO} (V)	Q_{rr}/Q_c (μC)
CAS300M12BM2 (Cree)	6x	1.7	3.2
SKM400GB125D (Semikron)	4x	1.1	45

are calculated at a load current of 300 A. In the Si IGBT, these losses are 2.2 times higher at 25 °C and 1.7 times higher at 125 °C compared to the SiC MOSFET. Furthermore, at the same load current, the ratio of on-state losses in Si diode to that in SiC diode is 1.25 at 25 °C and 0.99 at 125 °C. Due to the pure Ohmic characteristics of the MOSFET, the ratio of conduction loss in the Si IGBT to that in the SiC MOSFET is higher at lower current, indicating that the SiC MOSFET is more favourable than the Si IGBT. The converse is true for the switching loss because of the tail-current in the IGBT which causes non-linear behaviour of turn-off loss with load current.

The internal gate resistance (R_{gint}) in the MOSFET module is 3 Ω and in the IGBT module, it is 1.25 Ω. A higher value of R_{gint} limits the speed of the device.

III. SUMMARY OF MEASUREMENTS WITH VARYING GATE RESISTANCES

All the turn-on and turn-off switching transients are evaluated for a dc-link voltage of 600 V and a drain-source current of 300 A in each of the modules at 25 °C. Both the chosen modules are evaluated with varying gate resistance (R_g).

TABLE III
SUMMARY OF LABORATORY MEASUREMENTS FOR CAS300M12BM2 (CREE)

R_g (Ω)	dv/dt (V/ns)	di/dt (A/ns)	V_{os} (V)	I_{os} (A)	E_{on} (mJ)	E_{off} (mJ)	di/dt_1 (A/ns)
0	19.56	10.93	301	198	1.63	3.74	1.82
1	15.12	9.14	260	166	3.87	5.04	1.52
2.2	13.22	7.1	207	140	5.02	5.76	1.18
3.4	10.38	6.56	188	125	7.09	7.7	1.09
5	8.55	5.35	136	111	8.56	8.64	0.89
6.8	7.12	4.46	133	105	11.84	10.78	0.74
10	5.4	3.5	102	86	16.61	15.16	0.58
12	4.9	2.97	85	65	19.62	17.74	0.49

TABLE IV
SUMMARY OF LABORATORY MEASUREMENTS FOR SKM400GB125D (SEMIKRON)

R_g (Ω)	dv/dt (V/ns)	di/dt (A/ns)	V_{os} (V)	I_{os} (A)	E_{on} (mJ)	E_{off} (mJ)	di/dt_1 (A/ns)
0	16.64	12.2	233	393	3.94	7.68	3.04
1	13.23	9.07	270	279	11.9	8.87	2.26
2.35	9.8	5.7	296	168	24.9	10	1.42
3.9	7.32	3.58	276	118	36.2	12.15	0.89
4.7	6.57	3.05	270	108	40	13.62	0.76
6	5.21	2.41	236	89	49.5	16.4	0.60

The summary of the measurements taken during the experiments are listed in Table III and Table IV. dv/dt is the voltage slew rate during the turn-off, di/dt is the current slew rate per module, while di/dt_1 is the current slew rate per chip during the turn-on of the lower transistor. The R_g influences turn-on speed and thereby turn-on losses significantly. The details are explained along with the example waveforms in Section IV.

IV. COMPARISON OF SIC MOSFET AND SI IGBT

A. Similar dv/dt

The turn-off switching transients for the selected modules at similar dv/dt are illustrated in Fig. 4. The SiC MOSFET has lower turn-off losses compared to the Si IGBT, which is essentially due to the smaller voltage overshoot (V_{os}) in the SiC compared to the Si module.

However, the reduced losses in the SiC come with high frequency oscillations (26 MHz) as indicated in Fig. 4 a). V_{os} in the Si IGBT is higher compared to SiC MOSFET because of higher di/dt (10.8 A/ns) in the IGBT with regard to the MOSFET (7.97 A/ns). These oscillations and overshoots can be kept at an acceptable level either by reducing L_{stray}, or by slowing down the device. The former solution expedites further reduction in losses as well, while the latter results in increased switching losses as exemplified in Subsection F.

B. Similar di/dt per module

The anti-parallel diode in the Si IGBT module has a pn junction. Therefore, when the diode switches from the on-state to the reverse-blocking state, the current continues to flow until the stored charge within the drift region are swept out, which is referred as the reverse recovery phenomenon [17]. This negative current is added to the IGBT current during the turn-on of the IGBT, resulting in higher switching losses in the

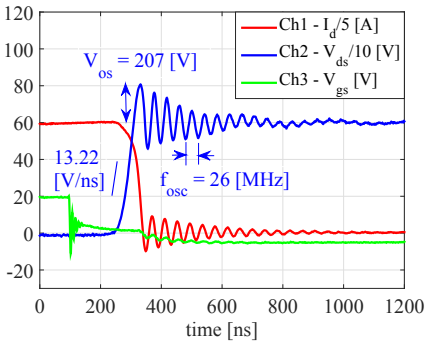

(a) Turn-off of CAS300M12BM2 (Cree). R_g = 2.2 Ω, E_{off} = 5.76 mJ, V_{os} = 207 V, di/dt = 7.97 A/ns.

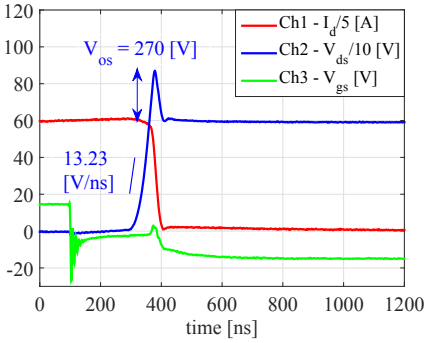

(b) Turn-off of SKM400GB125D (Semikron). R_g = 1 Ω, E_{off} = 8.87 mJ, V_{os} = 270 V, di/dt = 10.8 A/ns.

Fig. 4. Illustration of switching transients at similar dv/dt.

IGBT. The SiC MOSFET has SBD as an anti-parallel diode which has extremely low capacitive charge (Q_c). For instance, the reverse recovery charge (Q_{rr}) of the pn diode in the Si IGBT is higher by a factor of 14 compared to the Q_c of the SBD diode in the SiC MOSFET as presented in Table II.

The laboratory measurement shows that the turn-on switching energy loss is 3 times higher in the Si IGBT compared to the SiC MOSFET. The example waveforms with similar di/dt per module for the SiC MOSFET and the Si IGBT are depicted in Fig. 5.

C. Similar di/dt per chip

The Cree module has 6 chips in parallel whereas the Semikron has only 4. Fig. 6 exemplifies the turn-on transients at similar di/dt per chip. The turn-on energy loss is higher by a factor of 4.2 in the Si IGBT compared to the SiC MOSFET. Though the overshoots are similar in this case, the higher loss in the IGBT is caused mainly by the slower rise and fall time.

D. Similar voltage overshoot

The comparison of the case with similar V_{os} are illustrated in Fig. 7. The turn-off switching energy loss is higher by a factor of 1.76 in the Si IGBT compared to the SiC MOSFET. The tail current in IGBT functions partly as a turn-off snubber, resulting in lower or no ringing. However, the MOSFET is

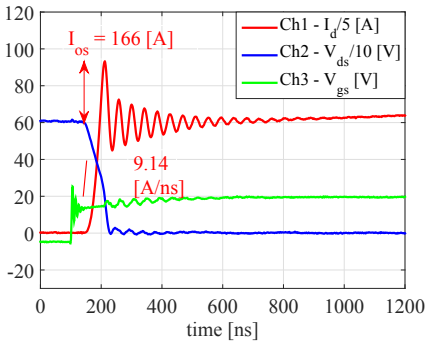

(a) Turn-on of CAS300M12BM2 (Cree). R_g = 1 Ω.

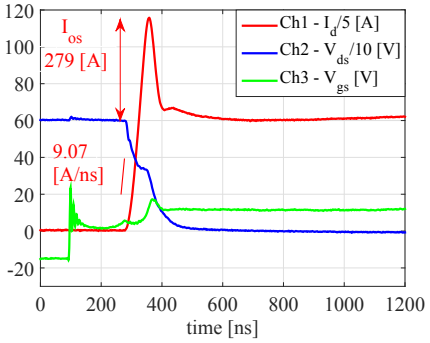

(b) Turn-on of SKM400GB125D (Semikron). R_g = 1 Ω, di/dt per chip area is 18.6 kA/ns/mm^2.

Fig. 5. Illustration of switching transients at similar di/dt per module.

a unipolar device and has no tail current so the amount of parasitic ringing is noticeably higher.

E. Similar current overshoot

The waveforms at similar current overshoot (I_{os}) are elucidated in Fig. 8. Laboratory measurements show turn-on losses of 3.87 mJ for the Cree and 24.9 mJ for the Semikron module, which is 6.4 times higher. Subsection C showing the waveforms at similar di/dt per chip also has almost similar I_{os}, where the losses were higher in the Si IGBT by a factor of 4.2 compared to the SiC. Nonetheless, the SiC MOSFET is slowed down to reduce ringings, it beats the Si IGBT in turn-on losses. Therefore, it is crucial to replace the Si anti-parallel diode with the SiC SBD in the Si IGBT module. Thereafter, the case temperatures of the IGBTs will be lower as a consequence of reduction in switching losses, which will not only improve the system efficiency by allowing the higher switching frequency and higher deliverable power, but also allow the reduction in chip size of the Si IGBTs.

F. Similar ringing during turn-off

The ringings during the turn-off are reduced using a higher R_g so that the losses can be compared between the selected modules. The laboratory measurement shows that turn-off loss in the SiC MOSFET is 2 times higher than the Si IGBT module in this case. However, one should not forget that the room temperature is not a real environment for a practical

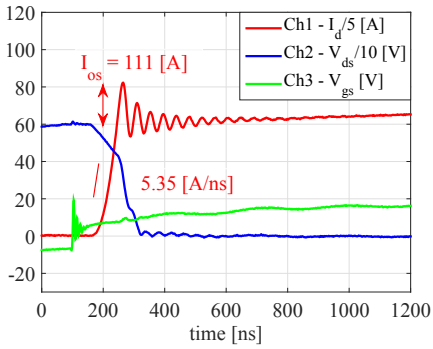

(a) Turn-on of CAS300M12BM2 (Cree). R_g = 5 Ω, E_{on} = 8.56 mJ, I_{os} = 111 A, di/dt per chip = 0.89 A/ns.

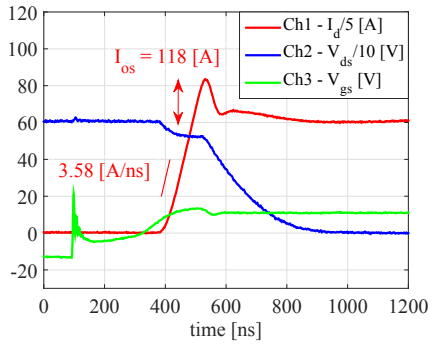

(b) Turn-on of SKM400GB125D (Semikron). R_g = 3.9 Ω, E_{on} = 36.2 mJ, I_{os} = 118 A, di/dt per chip = 0.89 A/ns.

Fig. 6. Illustration of switching transients at similar di/dt per chip.

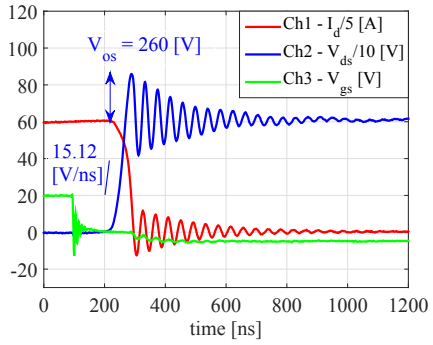

(a) Turn-off of CAS300M12BM2 (Cree). R_g = 1 Ω.

Fig. 7. Illustration of switching transients at similar V_{os}. Refer Fig. 4 b) for Semikron IGBT module in this case.

converter operation. The tail current in Si IGBT worsens with higher temperature, whereas the losses in SiC MOSFET increase a little or remain almost the same [5], [6].

G. Similar ringing during turn-on

The ringings during the turn-on are reduced by slowing down the SiC MOSFET module. The switching waveforms are displayed in Fig. 10. The turn-on energy loss in the Si IGBT is 1.2 times higher than that in SiC MOSFET. This demonstrates that the SiC MOSFET beats the Si IGBT in turn-on losses.

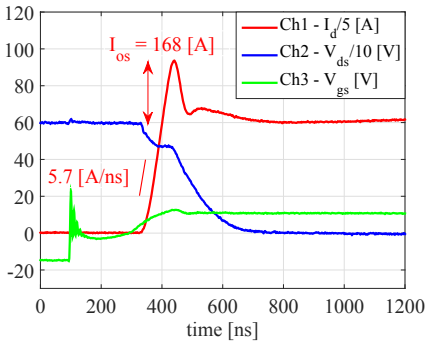

(a) Turn-on of SKM400GB125D (Semikron). R_g = 2.35 Ω.

Fig. 8. Illustration of switching transients at similar I_{os}. Refer Fig. 5 a) for Cree MOSFET module in this case.

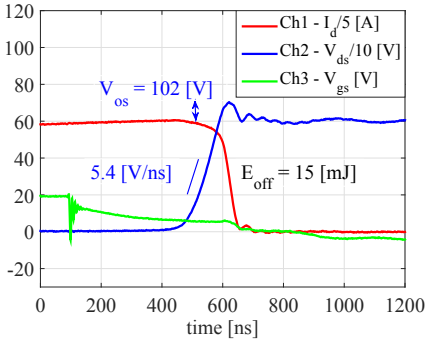

(a) Turn-off of CAS300M12BM2 (Cree). R_g = 10 Ω.

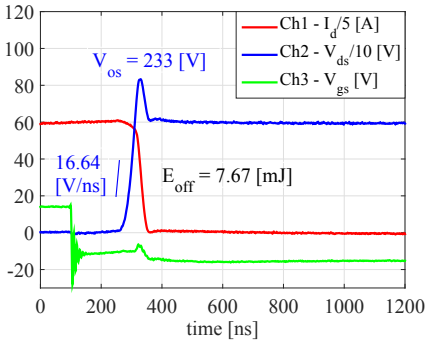

(b) Turn-off of SKM400GB125D (Semikron). R_g = 0 Ω.

Fig. 9. Switching transients during turn-off with similar ringing.

H. Summary of Section IV

The analysis of the switching losses in Section IV is summarized in Table V. For a given dc-link voltage and a load current, the switching energy loss depends on the overshoots and rise and fall time of the switching current and voltage.

It is explicitly clear that the SiC MOSFET has lower switching energy losses compared to the Si IGBT in all the cases except the case with similar ringing during turn-off. However, V_{os} in the Si IGBT is 38 %, while that in the SiC MOSFET is 17 % of the steady state voltage in the latter case.

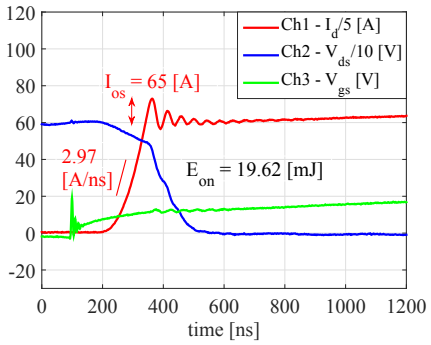

(a) Turn-on of CAS300M12BM2 (Cree). R_g = 12 Ω, di/dt per chip area is 19 kA/ns/mm^2.

Fig. 10. Switching transients during turn-on with similar ringing. Refer Fig. 8 a) for Semikron IGBT module in this case, where E_{off} = 24.9 mJ.

TABLE V
SUMMARY OF THE COMPARISONS FOR LOSS EVALUATION

Comparison Conditions	Si IGBT E (mJ)	SiC MOSFET E (mJ)	Improvement x
Similar dv/dt	8.87	5.76	1.54
Similar di/dt/module	11.9	3.87	3.0
Similar di/dt/chip	36.2	8.56	4.23
Similar V_{os}	8.86	5.04	1.76
Similar I_{os}	24.9	3.87	6.4
Similar ringing turn-off	7.68	15.16	0.5
Similar ringing turn-on	24.9	19.62	1.27

V. CHOICE OF GATE RESISTANCE

From Table IV, it is evident that V_{os} of the Si IGBT increases with R_{goff}, reaches a peak value and then decreases again. Therefore, R_{goff} of 0 Ω is chosen as an optimized value, which also gives lowest loss. As a trade-off between I_{os} and turn-on losses, R_{gon} of 2.35 Ω is chosen. The switching transients with R_{goff} of 0 Ω is exemplified in Fig. 9 b) and with R_{gon} of 2.35 Ω in Fig. 8 a). Considering ringings, switching losses and overshoots, R_{gon} of 5 Ω and R_{goff} of 3.4 Ω are chosen for the SiC MOSFET. The turn-on waveform is displayed in Fig. 6 a) and turn-off in Fig. 11.

Table VI shows the specific switching energy loss for the selected gate resistances. The turn-off loss turns out to be equal for both modules, whereas the turn-on loss in the SiC MOSFET is 1/3 times that of the Si IGBT. The specific reverse recovery loss of SiC diode is 1/8.76 times that of Si diode.

TABLE VI
SPECIFIC LOSS FOR THE SELECTED R_{gon} AND R_{goff}

Parts Half-bridge	R_{gon} (Ω)	R_{goff} (Ω)	E_{on-sp} (μJ/A)	E_{off-sp} (μJ/A)	E_{rr-sp} (μJ/A)
SiC MOSFET	5	3.4	28.5	25.6	1.3
Si IGBT	2.35	0	83	25.6	11.4

VI. DISCUSSION

With R_g of 0 Ω, the Cree module can switch at dv/dt of 19.6 V/ns during turn-off and di/dt of 10.9 A/ns during turn-on. The maximum speed of today's fast switching Si IGBT

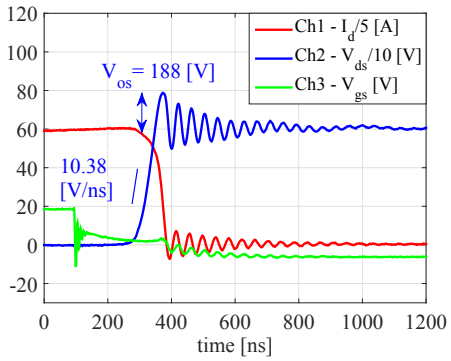

Fig. 11. R_g =3.4 Ω, di/dt = 8.2 A/ns, E_{off} = 7.7 mJ.

is 16.6 V/ns during turn-off and 12.2 A/ns during turn-on. The conduction loss in the SiC MOSFET is a factor of 0.45 and 0.58 at 25 °C and 125 °C respectively compared to the Si IGBT at a load current of 300 A. This fact explains that the SiC MOSFET competes even with the bipolar devices like Si IGBT with regard to conduction loss.

For the chosen R_g, the specific turn-off losses in both modules are similar, while the specific turn-on losses in the SiC MOSFET module is a factor of about 1/3 that of the Si IGBT at 25 °C. The real operating temperature of a converter is higher than the room temperature. The losses in the Si IGBT converter increases much more than in a SiC MOSFET converter because the tail current in the IGBT and Q_{rr} in the anti-parallel diode exhibit strong dependency on temperature. In the SiC MOSFET, the turn-on losses decrease and turn-off losses increase, and in overall the total losses slightly increase with increasing temperature as shown in previous work [6].

Moreover, the voltage overshoots are lower in the MOSFET compared to the IGBT. The turn-off losses in the MOSFET is 1/1.7 that of the IGBT, when both modules have similar V_{os}. These facts imply that the SiC MOSFET can replace the Si IGBT of the same or even higher voltage class.

The comparison with the similar ringings suggests that the SiC MOSFET beats the Si IGBT even in an application where lower dv/dt and switching frequency are required. With the reduced package and board parasitics, the SiC MOSFET becomes even more interesting, both in terms of switching speed and losses.

VII. Conclusion

The major conclusion derived from the comparative evaluation between the two modules are listed in the following 4 points.

i.) The highest achievable dv/dt is 19.5 V/ns and di/dt is 11 A/ns in the SiC MOSFET module. Similarly, in the Si IGBT module dv/dt is about 17 V/ns and di/dt is 12 A/ns. This information was missing in the datasheet of the modules.

ii.) The SiC MOSFET showed lower voltage overshoot while comparing the modules at similar dv/dt, enabling a further increase in the dc-link voltage, i.e., the SiC MOSFET can replace the Si IGBT even in higher voltage class.

iii) The turn-on losses are lower in the SiC MOSFET even in the case with similar ringings. The higher losses in the Si IGBT is primarily because of the higher Q_{rr} of the Si diode. Replacing this diode with the SiC SBD diode would lead to more proportionate turn-on losses between the two modules.

iv) The SiC MOSFET has lower conduction losses (a factor of 1/2.2 and 1/1.7 at 25 °C and 125 °C respectively at a load current of 300 A) compared to the Si IGBT, which strongly motivate in using unipolar SiC MOSFET instead of Si IGBT.

Thus, the lower switching energy losses in both faster and slower switching conditions, the lower conduction losses at all temperatures, and the smaller overshoots indicate that the SiC MOSFET can replace the Si IGBT.

Acknowledgment

The authors would like to thank The Research Council of Norway and 6 industry partners who sponsor this project: EFD Induction, Siemens, Eltek, Statkraft, Norwegian Electric Systems, and Vacon AS.

References

[1] M. O'Neill "Silicon carbide MOSFETs challenge IGBTs," App. Note, Cree, Inc., Durham, NC 27703, 2008.
[2] S. Davis "1200 V SiC MOSFET poised to replace Si MOSFETs and IGBTs," Power Electronics Technology, Feb. 2011.
[3] "The next generation of power conversion systems enabled by SiC power devices," White paper, Rohm Semiconductor, 2013.
[4] "SiC power devices and modules," App. Note, Rohm Semiconductor, Aug. 2014.
[5] S. Tiwari, O. -M. Midtgård, T. M. Undeland, and R. Lund "Experimental performance comparison of six-pack SiC MOSFET and Si IGBT modules paralleled in a half-bridge configuration for high temperature applications," Wide Bandgap Power Devices and Applications (WiPDA), 2015 IEEE 3^{rd} Workshop on, Blacksburg, VA, 2015, pp. 135-140.
[6] S. Tiwari, O. -M. Midtgård and T. M. Undeland, "SiC MOSFETs for Future Motor Drive Applications," Power Electronics and Applications (EPE'16 ECCE-Europe), 2016 18^{th} European Conference on, Karlsruhe, 2016, pp. 1-10.
[7] K. Vechalapu, S. Bhattacharya, E. Van Brunt, Sei-Hyung Ryu, D. Grider and J. W. Palmour, "Comparative evaluation of 15 kV SiC MOSFET and 15 kV SiC IGBT for medium voltage converter under same dv/dt conditions," Energy Conversion Congress and Exposition (ECCE), 2015 IEEE, Montreal, QC, 2015, pp. 927-934.
[8] S. Tiwari, I. Abuishmais, T. Undeland and K. Boysen, "Silicon carbide power transistors for photovoltaic applications," PowerTech, 2011 IEEE Trondheim, Trondheim, 2011, pp. 1-6.
[9] S. Tiwari, T. Undeland, S. Basu and W. Robbins, "Silicon carbide power transistors, characterization for smart grid applications," Power Electronics and Motion Control Conference (EPE/PEMC), 2012 15^{th} International, Novi Sad, 2012, pp. LS6d.2-1-LS6d.2-8.
[10] S. Tiwari, O. -M. Midtgård and T. M. Undeland, "Design of low inductive busbar for fast switching SiC modules verified by 3D FEM calculations and laboratory measurements," 2016 IEEE 17^{th} Workshop on Control and Modeling for Power Electronics (COMPEL), Trondheim, Norway, 2016, pp. 1-8.
[11] S. Tiwari, A. Rabiei, P. Shrestha, O. -M. Midtgård, T. Undeland, R. Lund, A. Gytri, "Design considerations and laboratory testing of power circuits for parallel operation of silicon carbide MOSFETs," Power Electronics and Applications (EPE'15 ECCE-Europe), 2015 17^{th} European Conference on, Geneva, 2015, pp. 1-10.
[12] "SiC MOSFET Isolated Gate Driver," App. Note, CPWR-AN10 Rev. C, Cree, Inc., Durham, 2014.
[13] "CAS300M12BM2 Datasheet," Cree, Inc., 2014.
[14] "SKM400GB125D Datasheet," Semikron, Inc., 2007.
[15] "SIGC121T120R2CS Datasheet," Infineon, Inc., 2003.
[16] "CPM212000025B Datasheet," Cree, Inc., 2016.
[17] J. B. Baliga, Fundamentals of power semiconductor devices, 2008, pp. 236.